Metrologia 56 (2019) 025005 (15pp) https://doi.org/10.1088/1681-7575/aafced

Improving two-way satellite time and frequency transfer with redundant links for UTC generation

Zhiheng Jiang[1], Victor Zhang[2,6], Thomas E Parker[2], Gérard Petit[1], Yi-Jiun Huang[3], Dirk Piester[4] and Joseph Achkar[5]

[1] BIPM, Bureau International des Poids et Mesures, Sévres, France
[2] NIST, National Institute of Standards and Technology, 325 Broadway, Boulder, CO 80305, United States of America
[3] TL, National Standard Time and Frequency Laboratory, Telecommunication Laboratories, Chunghwa Telecom, Chinese Taipei
[4] PTB, Physikalisch-Technische Bundesanstalt, Bundesallee 100, 38116 Braunschweig, Germany
[5] OP, LNE-SYRTE, Observatoire de Paris, Université PSL, CNRS, Sorbonne Université, 61 avenue de l'Observatoire, 75014 Paris, France

E-mail: victor.zhang@nist.gov

Received 13 August 2018, revised 1 January 2019
Accepted for publication 9 January 2019
Published 22 February 2019

Abstract

Two-way satellite time and frequency transfer (TWSTFT) is a primary technique for the generation of coordinated universal time (UTC). At present, more than 12 timing laboratories around the world use SAtellite Time and Ranging Equipment (SATRE) modems in TWSTFT operations and contribute data for the realization of UTC. The advantages of TWSTFT are its small calibration uncertainty ($\leqslant$1.0 ns if the link is calibrated with a TWSTFT mobile station) and its long-term link stability. However, the precision of SATRE TWSTFT in the operational networks is degraded by a daily variation pattern (diurnal) in the TWSTFT results. The diurnal with varying amplitude appears virtually in all SATRE TWSTFT links. The observed peak-to-peak variation of the diurnals can reach 2.0 ns in some cases. So far, studies on the sources of the diurnal have not provided conclusive understanding of the diurnal's dominant origin.

Therefore, efforts have been made to reduce the impact of the diurnal variation in TWSTFT for UTC computation. The BIPM has been using the combination of SATRE TWSTFT results and GPS carrier-phase precise point positioning solutions (GPSPPP) for UTC computation since 2010. The combination adjusts the GPSPPP results to long-term averages of TWSTFT and is effectively free from the diurnal variations because the GPSPPP results contain almost no diurnal. Lately, the use of software-defined radio receivers (SDR) in TWSTFT has shown one way of how to reduce the diurnal variations by a factor of two to three in most of the inner-continental SATRE TWSTFT links, and furthermore, how the short-term stability for all UTC SDR TWSTFT links can be improved. In addition, there has been research on the full use of the redundancy in the TWSTFT network to improve the TWSTFT link stability. Recent studies on evaluating indirect links revealed that it is possible to apply a simplified procedure to use the redundancy, in a most effective way, to reduce the diurnal variations in the Europe-to-Europe SATRE TWSTFT links by a factor of two to three. Based on these findings, we gained new insights about the diurnals and its dominant origin(s) which are discussed in this paper. The methods of the combination of SATRE TWSTFT and GPSPPP as well as the indirect SATRE TWSTFT links utilize the redundancy in the UTC time transfer network. SDR TWSTFT can largely reduce the diurnal in SATRE TWSTFT, but noticeable residual

[6] Author to whom any correspondence should be addressed.

diurnal remains. In this paper, we provide the analyses of using the combination of SDR TWSTFT and GPSPPP results, as well as using the indirect SDR TWSTFT links. This paper concludes that the use of SDR TWSTFT redundant links can further improve the stabilities of UTC TWSTFT links. In addition, the use of SDR TWSTFT indirect links is a pure TWSTFT solution. The independence of the TWSTFT results to GPS results can improve the robustness of UTC computation.

Keywords: TWSTFT, diurnal, SDR, indirect link, combination of TWSTFT and GPS, redundancy, stability

(Some figures may appear in colour only in the online journal)

List of acronyms and specific terms

BIPM	Bureau International des Poids et Mesures
AOS, CH/METAS, IT/INRIM, NIST, NPL, OP/LNE-SYRTE, PTB, ROA, SP/RISE, USNO, VSL	Acronyms of UTC laboratories
AOS	Astrogeodynamic Observatory, Poland
CH/METAS	Federal Institute of Metrology METAS, Switzerland
IT/INRIM	Istituto Nazionale di Ricerca Metrologica, Italy
NIST	National Institute of Standards and Technology, USA
NPL	National Physical Laboratory, United Kingdom
OP	Observatoire de Paris, France
PTB	Physikalisch-Technische Bundesanstalt, Germany
ROA	Real Instituto y Observatorio de la Armada, Spain
SP/RISE	Research Institutes of Sweden, Sweden
USNO	United States Naval Observatory, USA
VSL	Dutch Metrology Institute, Netherlands
1 PPS	One pulse per second
BPSK	Binary phase-shift keying
KCDB	BIPM key comparison data base CCTF-K001.UTC
CCTF	Consultative Committee for Time and Frequency
DCD	Double Clock Difference, the difference between two time links which are connected to the same clocks at both ends
Diurnal	A daily variation pattern apparent in the TWSTFT results, dominant uncertainty source in SATRE TWSTFT
Gain factor or Gain	A measure quantifying the improvement between two time series A and B as the ratio σ(A)/σ(B) or σ_x(A)/σ_x(B). If Gain $>$ 1, we define that B is improved over A
GPSPPP or PPP for short	GPS carrier-phase precise point positioning solution for time and frequency transfer
GPSIPPP or IPPP for short	GPS carrier-phase integer ambiguity PPP solution for time and frequency transfer
IF	Intermediate frequency (~70 MHz)
Ku-band	Frequency band (10.7–14.5 GHz) used for space radiocommunications
Lab1_Lab2^Lab3 or Lab1_Lab2^ or Link^Lab3 or Link^	an *indirect* TWSTFT link between Lab1 and Lab2 via Lab3. ^ is the indirect link operator, e.g. OP_PTB^NIST is the indirect link between OP and PTB via NIST. It can be further divided accordingly into Link$^{\wedge}_{\mathrm{SATRE}}$ or Link$^{\wedge}_{\mathrm{SDR}}$. Similarly, we define DCD$^{\wedge}_{\mathrm{SATRE}}$ or DCD$^{\wedge}_{\mathrm{SDR}}$ as the DCD of indirect SATRE or SDR link
MJD	Modified julian date
PDD	Path delay difference
PRN	Pseudorandom noise
SATRE	SAtellite Time and Ranging Equipment, brand name of a modem developed by Time Tech GmbH, Stuttgart, Germany
SATRE TWSTFT, SATRE link or SATRE for short	TWSTFT using the SATRE modems
SDR TWSTFT, SDR link or SDR for short	TWSTFT with measurements made by software-defined radio receivers
TWSTFT or TW for short	Two-way satellite time and frequency transfer
TW $\oplus$ PPP or Link $\oplus$	A combination of TWSTFT and PPP. $\oplus$ is the combination operator. It can be further divided accordingly into SATRE $\oplus$ PPP and SDR $\oplus$ PPP
u_A, u_B	Type A and B uncertainties
UTC	Coordinated universal time
WG on TWSTFT	CCTF working group on TWSTFT
σ(A)	Standard deviation of a time series A
σ_x(A) or TDev(A)	Time deviation of a time series A, expressed in seconds

1. Introduction

Since 2003, two-way satellite time and frequency transfer (TWSTFT) has been used as a primary time transfer technique for the realization of coordinated universal time (UTC) [1–3]. As of today, TWSTFT is based on pseudorandom noise (PRN) code measurements. Each TWSTFT station transmits a PRN signal modulated via binary phase-shift keying (BPSK) onto a Ku-band carrier frequency. In the transmitting part of the modem, the BPSK sequence of a PRN code is generated and the phase modulation is synchronized with the local clock's one pulse per second (1 PPS) output. Each TWSTFT

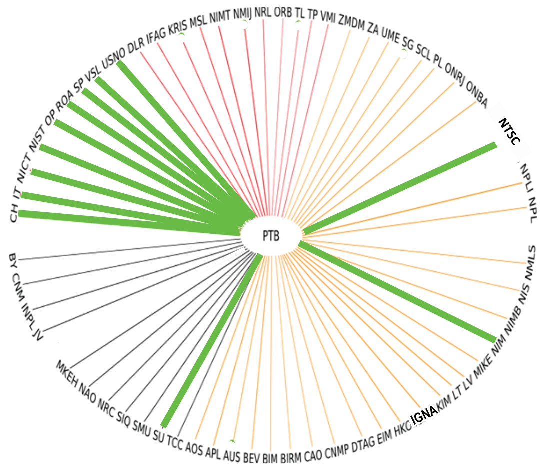

Figure 1. Configuration of the UTC time transfer network with PTB as the pivot point. As of 2017, there are 12 TWSTFT links (green) and 65 GPS time transfer links (other colours) used in the UTC generation. For each TWSTFT link, there is also a parallel GPS link available. The TWSTFT and GPS links over the same baseline are redundant to each other.

station uses a dedicated PRN code for its BPSK sequence in the transmitted signal. In the receive part of the modem, the BPSK sequence of the remote station is generated and correlated with the received signal. As a result, the time-of-arrival of the received signal is obtained with respect to the local clock. Presently all TWSTFT stations contributing to UTC are equipped with SATRE modems. In the last 15 years, diurnals with varying amplitude have been observed in all links using different communication satellites with different chip-rates and between TWSTFT stations at different and far distributed locations. They are the dominant source of TWSTFT short-term instability, with peak-to-peak amplitudes of up to 2 ns in the case of the widely used BPSK modulations of 1 MChip/s. Great efforts have been made in the investigations of the sources of the diurnals and unfortunately no major progress has been obtained in the past one and half decades, see e.g. [5, 18, 19]. Up to now, we still do not know the dominant origin of the diurnals. One major contributor to the diurnals, however, could be related to properties of the receive part in the SATRE modem.

Nevertheless, the BIPM and the TWSTFT community are focused on reducing the impact of the diurnals in the SATRE TWSTFT results for UTC. The principle idea is to best use the rich redundancy in the worldwide UTC time transfer network, which is shown in figure 1. We will refer to the clock comparisons between two laboratories as a time transfer baseline and the time transfer technique used over the baseline as a time transfer link. For example, time transfer between PTB and OP is a baseline and TWSTFT between PTB and OP is a link.

There are three methods fully developed and applicable to reduce the diurnals that have produced encouraging results.

(i) Combination of TWSTFT and GPSPPP: In 2009, the use of the combination of SATRE TWSTFT results and GPSPPP solutions, here referred to as TW $\oplus$ PPP, was proposed for UTC computation [6]. This approach is possible because for each TWSTFT link a GPS link exists over the same baseline. The GPSPPP is based on the phase measurements of GPS carrier frequency. The GPS code measurements are also used to resolve the carrier frequency cycle ambiguity. Because the GPS carrier frequencies are much higher than the chip-rate of the PRN codes for either GPS or TWSTFT signals, the GPSPPP can achieve much higher precision. The phase measurements also seem to be less affected by effects with diurnal signatures. However, GPSPPP solutions contain data boundary discontinuities due to the noise of the code measurements used to estimate the phase ambiguities over the computation batch. In recent years, several techniques have been developed to mitigate the GPSPPP data boundary discontinuity, such as IPPP and the revised RINEX-shift (RRS) algorithm [24]. However, these techniques are either still under development or not validated by the BIPM for use in UTC computation. TW $\oplus$ PPP combines the advantages (mainly the calibration with $u_B \leqslant 1$ ns and the typical long-term stability in TWSTFT [25] together with high precision and diurnal-free GPSPPP) and reduces the disadvantages (mainly the diurnal in SATRE TWSTFT and the data boundary discontinuity in GPSPPP) of the two methods. The BIPM began using it for UTC computation and publishing results in both Circular T [1] and KCDB [22].

(ii) Use of software-defined radio (SDR) receivers in TWSTFT: In 2016, it was demonstrated that bypassing the receive part of SATRE modems and using SDR receivers for TWSTFT measurements at IF (SDR TWSTFT) could considerably reduce the diurnals and the measurement noise [7–9]. In the current configuration, an SDR receiver operates in parallel with a SATRE modem, and therefore, the SATRE and SDR TWSTFT data are redundant. In each station, the transmission signal is generated by a SATRE modem and the down-converted received signal is split and fed to both the SDR setup and SATRE modem. The arrival time of the signal is thus determined by the SATRE modem and SDR receiver independently [9]. With SDR TWSTFT, the diurnals in most of the inner-continental (such as the Europe-to-Europe and Asia-to-Asia) SATRE TWSTFT links are reduced by a factor of two to three and we obtain a gain in stability for all UTC SDR TWSTFT links. Because of the diurnal and short-term noise reduction [9], we believe the uncertainty of SDR TWSTFT link calibration should be smaller than that of the SATRE TWSTFT link calibration (with $u_B \leqslant 1$ ns). To assess the actual uncertainty of SDR TWSTFT link calibration, the CCTF WG on TWSTFT and the SDR TWSTFT participating stations are working on the SDR TWSTFT link calibration. At its 21st meeting in 2017, the CCTF endorsed the recommendation of its WG on TWSTFT [4] to work towards implementing the use of SDR TWSTFT data in UTC generation. The BIPM has used SDR TWSTFT as a backup technique for the UTC since October 2017 and is working towards applying it to both Circular T and the single Key Comparison for time and frequency. However, diurnals are not completely removed in SDR TWSTFT, especially for the inter-continental TWSTFT links, and the residual diurnal is

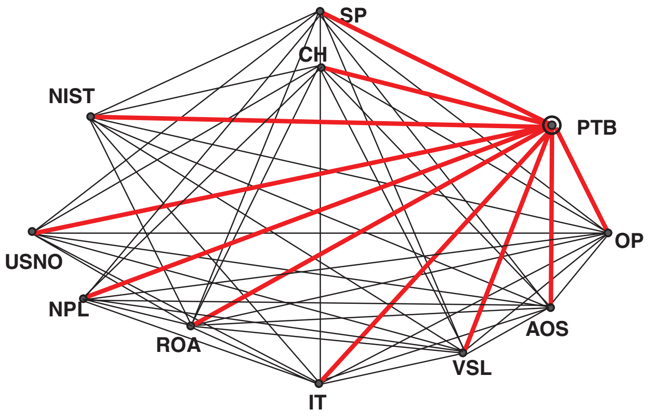

Figure 2. Status of the Europe-to-Europe and Europe-to-USA TWSTFT networks as of July 2018. There are 11 participating laboratories with a total of 52 links (NPL does not operate transatlantic TWSTFT and there is no direct link between NIST and USNO). The 10 UTC links are shown by the red lines with PTB.

still the dominant part in the uncertainty budget in the SDR TWSTFT.

(iii) Use of indirect TW links: In 2008, the TWSTFT network time transfer technique was proposed to fully use the redundancy in the TWSTFT network [10, 11]. This method, however, in many cases, does not provide a significant gain in reducing diurnal as given by the methods (i) and (ii). Therefore, the study ceased for nearly 10 years until new findings appeared recently [12, 13]. The findings revealed that some indirect links in a TWSTFT network may reduce the diurnals with respect to the direct links, and a gain factor of three to five can be attained.

This paper investigates the following points related to the three methods above:

– To which level methods (i) and (iii) can reduce the residual diurnals in TWSTFT;
– To which level methods (i) and (iii) can improve the stabilities of both SATRE TWSTFT and SDR TWSTFT by significantly reducing the diurnal;
– To compare the three methods in view of UTC time transfer;
– To analyse possible dominant causes of diurnals in Europe-to-Europe TWSTFT from the results obtained by methods (ii) and (iii).

We present our analyses using examples of the Europe-to-Europe and the Europe-to-USA links, especially the OP-PTB links. The choice of examples is based on the facts (1) the links have the most continuous and complete data sets (SATRE, SDR, GPSPPP and IPPP); (2) there is no satellite change since 2011; and (3) the indirect link method only works satisfyingly in the Europe-to-Europe links with a relay station in the USA. In section 2, we first briefly discuss previous results on the redundancy in the UTC time transfer network and on the evidence of residual diurnals in SDR TWSTFT, and present the tools to be used in our analysis. Then, in section 3, we present the SDR $\oplus$ PPP results based on method (i), the combination of TWSTFT and GPSPPP, to improve the SDR TWSTFT and, in section 4, we present the indirect TWSTFT links' results based on method (iii). In section 5 we compare all methods in their effect on reducing diurnal residuals and in section 6 we analyse and discuss the nature of diurnals in TWSTFT. Section 7 summarizes our study.

2. Key issues in the redundant link study

2.1. The redundancy in the UTC time transfer network

As shown in figure 1, the UTC time transfer network is comprised of mainly TWSTFT and GPS links. If both links are available over the same baseline, they are redundant. Before 2010, the primary time transfer technique policy was applied to the generation of UTC. This means only one of the TWSTFT and GPS techniques was used to compute an UTC link. Since 2010, the combination TW $\oplus$ PPP (or more specific SATRE $\oplus$ PPP) enables the use of the redundancy in UTC generation [6]. In fact, the same procedure as used for SATRE $\oplus$ PPP can be used for SDR $\oplus$ PPP.

Each TWSTFT network is highly redundant. In general, for a N-node network, there are $N(N-1)/2$ TWSTFT links. Among them, only $N-1$ links are being used for UTC. Figure 2 shows an example of the Europe-to-Europe and Europe-to-USA TWSTFT networks. A network time transfer method [10–11, 14] was proposed to fully use all the available links for UTC time transfer. It works very well in reducing the measurement noise but is not effective for the diurnal, a non-white noise process. On the other hand, each of the $N-1$ UTC links (Lab1 − Lab2) can also be obtained from the $N-2$ indirect non-UTC links, which make the use of one relay station (Lab3) in the network with no extra measurements (Lab1_Lab2^Lab3 = Lab1 − Lab3 + Lab3 − Lab2). Studies [12, 13] showed that certain indirect links can achieve a reduction of both measurement noise and diurnals.

2.2. Residual diurnal in SDR TWSTFT

Figure 3 shows the SDR TWSTFT difference over the baseline of OP-PTB. It has been demonstrated [7–9], that the OP-PTB SDR TWSTFT link is one of the most improved links where the diurnal is reduced by a factor of 3.7. However, as can be seen in the plot, a noticeable residual diurnal signal still exists with a peak-to-peak amplitude about 0.4 ns. This suggests that eliminating the residual diurnal will further improve the stability of the SDR TWSTFT links. The most recent study on SDR TWSTFT [9] found when the peak-to-peak diurnal variation in SATRE TWSTFT link is about 0.4 ns or less, the SDR TWSTFT hardly removes any amount of diurnal.

2.3. The data sets and analysis tools

Our analysis is based on comparisons of different techniques (time links) operated in parallel over a given baseline. In this way, the properties of the clocks are common in each link and are removed by computing double clock differences (DCD). The data sets (links) used in this study include: SATRE, SDR,

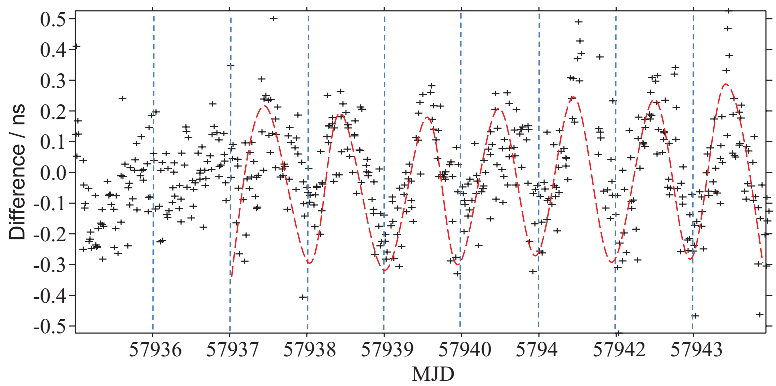

Figure 3. A noticeable residual diurnal remained in the SDR TWSTFT difference over the baseline of OP-PTB.

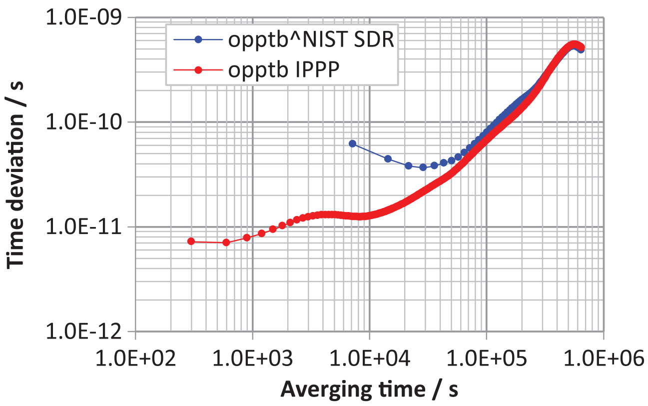

Figure 4. TDev of the IPPP and the indirect SDR link OP_PTB^NIST over the baseline of OP-PTB. Data during MJDs 58085–58115 are used in the computation. The five min IPPP data are taken from the BIPM time link comparison file for 1712. The small bump in the IPPP TDev at averaging time around 3000 s might be associated the errors in solving the ambiguities for each GPS satellite pass.

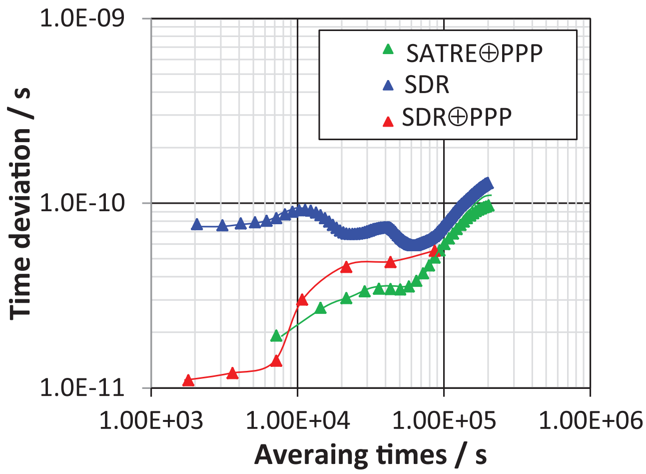

Figure 5. TDev of the SDR link and the SDR ⊕ PPP link over the baseline of OP-PTB.

PPP, GPS integer ambiguity PPP solutions (IPPP) [15], the combination of TWSTFT and GPSPPP (TW ⊕ PPP) and indirect links (Lab1_Lab2^Lab3). The DCD analysis has been made over selected baselines between (a) the SATRE and the SDR TWSTFT links, and (b) the SATRE and/or SDR TWSTFT against GPS PPP and/or GPS IPPP links.

The analysis employs the following statistical measurands:

- Time deviation (TDev), σ_x [17], of time links, standard deviation and time deviation of double clock difference, σ(DCD) and σ_x(DCD);
- The following two indicators are used for assessment of the quality and the level of the improvement:

1. σ_x for evaluation of the time link instabilities at different averaging times (τ);
2. σ(DCD) for revealing the agreement of the two types of links.

- Gain factors of link *Type2* versus link *Type1*: the ratio of σ(*Type1*)/σ(*Type2*) or σ_x(*Type1*)/σ_x(*Type2*).

For DCD comparisons of TWSTFT to GPS links, IPPP solutions are the preferred reference. Indeed, contrary to the standard PPP that solves the ambiguities of GPS carrier phase signals as real number values, IPPP solves them as integer cycles in accordance of their physical properties. This removes errors associated with solving real number ambiguities in PPP solutions, which may sum up as random walk instability over the computation batch. In comparison to independent high-performance techniques such as fiber links and TW carrier phase [15, 16], it has been found that IPPP is diurnal free and is the most precise of the presently available GPS comparison techniques. The short-term instability of IPPP is evidently superior to the short-term instability of IPPP is evidently superior to the code-based TWSTFT techniques considered in this study. As an example, figure 4 is a comparison of the TDev, $\sigma_x(\tau)$, of IPPP against the indirect SDR link OP_PTB^NIST over the baseline of OP-PTB. As seen, the IPPP link is more stable than the SDR link^ for averaging times up to one day. Therefore, we use IPPP when possible as a reference in the DCD comparisons of this study and only when it is not available we use PPP.

3. Improvement from the combination of TWSTFT and GPS: SDR ⊕ PPP

In this section, we study how to minimize or eliminate the residual diurnal in SDR TWSTFT by using the combination of SDR TWSTFT results and GPS PPP solutions, SDR ⊕ PPP. The technique of SATRE ⊕ PPP has been used in UTC

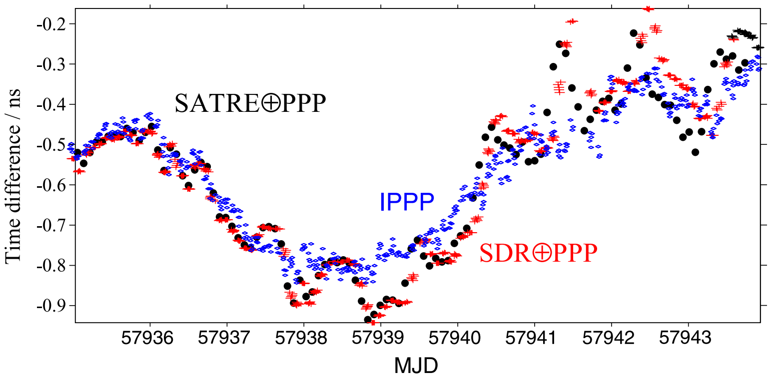

(a)

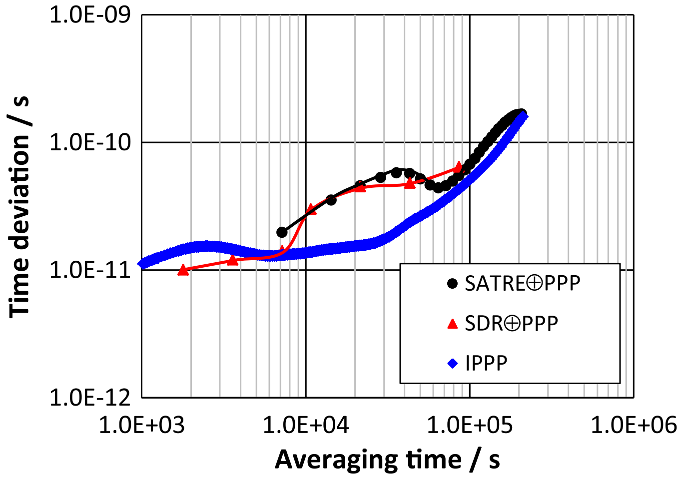

(b)

Figure 6. (a) The IPPP link (blue) versus the SDR ⊕ PPP link (red) and SATRE ⊕ PPP link (black) over the baseline of OP-PTB. (b) TDev of the IPPP link versus the SDR ⊕ PPP link and SATRE ⊕ PPP link corresponding to the data in figure (a). The short-term stability of both SATRE ⊕ PPP and SDR ⊕ PPP is very similar, that is dominated by the stability of the PPP solution.

Table 1. Gain of SDR ⊕ PPP link relative to SDR link over the baseline of OP-PTB.

DCD	No	Min/ns	Max/ns	Mean/ns	σ(DCD)/ns	Gain factor
SDR-IPPP	524	0.198	1.247	0.721	0.158	
(SDR ⊕ PPP)-IPPP	524	0.547	1.004	0.725	0.078	**2.0**

computations for nearly 10 years. The SDR ⊕ PPP is based on the same mathematical model as SATRE ⊕ PPP and the processing of SDR ⊕ PPP uses the same BIPM UTC software package Tsoft. The only difference between SATRE ⊕ PPP and SDR ⊕ PPP is the use of SATRE data or SDR data, respectively. For mathematical details on the combination technique, please refer to [6]. In the BIPM standard solutions, the epochs of GPS PPP or IPPP results are on a five min or 30 s grid, respectively, while the SDR TWSTFT measurements are grouped into several five min sessions made bi-hourly. In our analysis below, we interpolate the PPP/IPPP solutions to the epochs of SDR TWSTFT results, typically separated by about 15 to 30 min.

Figure 5 shows the TDev of the SDR and the SDR ⊕ PPP links over the baseline of OP-PTB. We see a clear residual diurnal at averaging times around 40 000 s in the TDev for SDR link. This diurnal is significantly reduced in the TDev of the SDR ⊕ PPP link. At this time, we do not know the origin of the small bump in the TDev for SDR at averaging times around 10 000 s.

Figures 6(a) and (b) show the performance of the IPPP link versus the SDR ⊕ PPP link and their corresponding time deviations. The SATRE ⊕ PPP link and its TDev are also included as a comparison. In figure 6(b), we see both IPPP and SDR ⊕ PPP links have excellent stability. The SDR ⊕ PPP solution seems marginally more stable than the IPPP solution for averaging times less than two hours. The IPPP is more stable than the SDR ⊕ PPP in averaging times of more than two hours which may be associated at least partly to the errors in solving real valued ambiguities for each GPS satellite pass in PPP.

We use IPPP as a reference in computation of DCDs to evaluate the gain of the SDR ⊕ PPP link over the SDR link for the baseline of OP-PTB. Table 1 presents the result. In the table, the 'Min' and 'Max' are the minimum and maximum values of the DCDs. The 'Gain factor' is the ratio of the σ[DCD(SDR-IPPP)] and σ[DCD(SDR ⊕ PPP-IPPP), i.e. 0.158 ns/0.078 ns = 2.0.

With this result, we show that the diurnal in SDR ⊕ PPP is further reduced with respect to SDR and the stability is

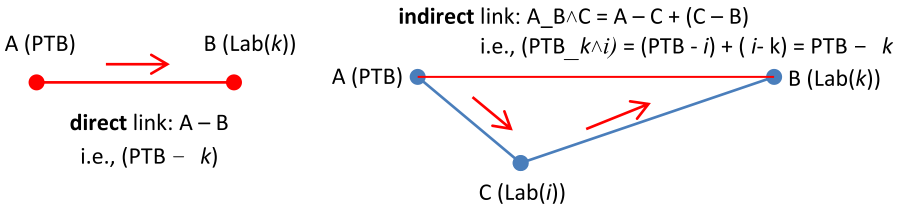

Figure 7. The direct link (left) and indirect link^i between PTB and lab(k) via lab(i) (right).

Table 2. DCD of Link and Link^ via USNO and NIST.

Baseline	N	DCD (Link–Link^NIST) mean/σ (ns)	DCD (Link–Link^USNO) mean/σ (ns)
CH-PTB	335	0.305 / 0.586	0.228/0.608
IT-PTB	365	−0.163/0.835	0.054/0.822
OP-PTB	355	−0.062/0.451	−0.069/0.553
ROA-PTB	335	0.268/0.811	0.250/0.793
SP-PTB	360	0.249/0.453	0.188/0.523
VSL-PTB	370	−0.462/0.567	−0.455/0.785
Mean		**0.022/0.617**	**0.033/0.681**

significantly improved by a factor of two. Considering that the reference IPPP is not errorless, the true gain factor may even be somewhat larger. The same is true in the following discussions.

4. Improvement from the TWSTFT indirect links

As mentioned in section 2.1, UTC TWSTFT networks contain a rich redundancy based on the current use of TWSTFT data in UTC computation. For a TWSTFT network with N participating stations, we have $N-1$ direct UTC links among all the available $N(N-1)/2$ links. On the other hand, each of the $N-1$ UTC links can also be obtained from $N-2$ indirect links, which make the use of one relay station in the network with no extra measurements. However, not all the indirect links can bring us the benefit of improving TWSTFT stability. In this section, we show that Europe-to-Europe SATRE and SDR TWSTFT indirect links with one station in the USA take advantage of the TWSTFT network redundancy to improve the stability of the Europe-to-Europe UTC TWSTFT links. We first present the calibration consistency of all UTC and non-UTC, direct and indirect links used in the study in section 4.2.1. The calibrations of the direct and indirect links should be consistent with each other. In section 4.2.2, we study the role of the relaying TWSTFT stations of the indirect links, and we use the tools given in section 2.3 and additionally a fast Fourier transform (FFT) analysis to compute the gain factors in diurnal reduction. We compare the gains in SATRE and SDR TWSTFT in section 4.3. In general, the time transfer quality of a Europe-to-USA or transatlantic link is better than that of a Europe-to-Europe link in terms of the magnitude of diurnal and noise. We provide a possible explanation on that in section 6.

*4.1. Definition of an indirect link: link^*

Let A – B denote a direct link over the baseline between laboratories A and B as shown on the left in figure 7, where the baseline is between PTB and Lab(k). To date, all UTC links are direct and therefore the shortest. In 2008, the concept of an indirect link was defined [10]. An indirect link between A and B is the link relayed via lab$C$ (Lab(i) in the drawing on the right in figure 7: A_B^C = A − C + (C − B). For example, using NIST as the relaying laboratory, we can obtain the indirect link between PTB and OP, i.e. PTB_OP^NIST = (PTB – NIST) + (NIST – OP). We use Lab1_Lab2^Lab3 or Link^ to represent an indirect link between Lab1 and Lab2 via Lab3, where ^ is the indirect link operator. Furthermore, we use Link$^{\wedge}{}_{\mathrm{SATRE}}$ or Link$^{\wedge}{}_{\mathrm{SDR}}$ to label the indirect link computation with SATRE or SDR TWSTFT data, respectively.

Owing to the law of propagation of uncertainties, one would expect that a direct link should result in a smaller uncertainty than that of the indirect link. However, the studies on the indirect TWSTFT links [12, 13] showed this is not always true due to the presence of significant non-white noise and other significant uncertainty contributions in some links as discussed in section 6.

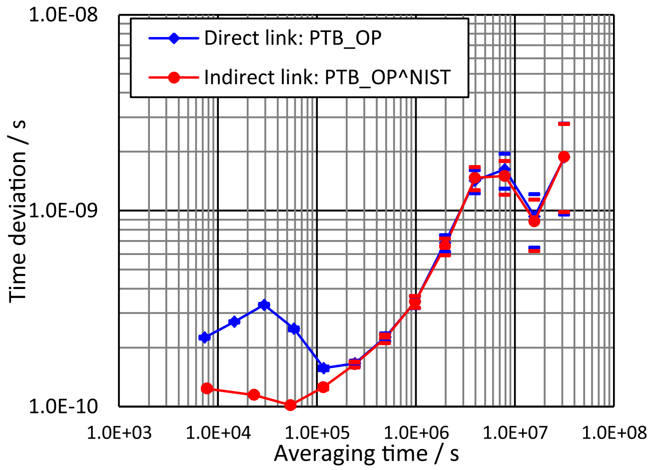

Figure 8. TDev of the direct (blue) and indirect (red) links over the baseline of OP-PTB. Data are taken from [12].

Table 3. (a) Gain in TDev of the TWSTFT direct link (**CH** – **PTB**) versus the indirect links via NIST or USNO. (b) Gain in TDev of the TWSTFT direct link (**OP** – **PTB**) versus the indirect links via NIST or USNO.

(a)

Averaging times (h)	Link σ_x/ns	Link^NIST σ_x/ns	Link^USNO σ_x/ns	Gain^NIST = (2)/(3)	Gain^USNO = (2)/(4)
(1)	(2)	(3)	(4)	(5)	(6)
2	0.39	0.14	0.21	2.8	1.9
4	0.34	0.13	0.14	2.6	2.4
8	0.52	0.09	0.11	5.8	4.7
16	0.23	0.11	0.14	2.1	1.6
32	0.21	0.18	0.21	1.2	1.0
Mean				**2.9**	**2.3**

(b)

Averaging times (h)	Link σ_x/ns	Link^NIST σ_x/ns	Link^USNO σ_x/ns	Gain^NIST = (2)/(3)	Gain^USNO = (2)/(4)
2	0.33	0.13	0.12	2.8	2.8
4	0.36	0.12	0.11	3.0	3.3
8	0.19	0.06	0.06	3.2	3.2
16	0.14	0.07	0.07	2.0	2.0
32	0.13	0.07	0.06	1.9	2.2
Mean				**2.6**	**2.7**

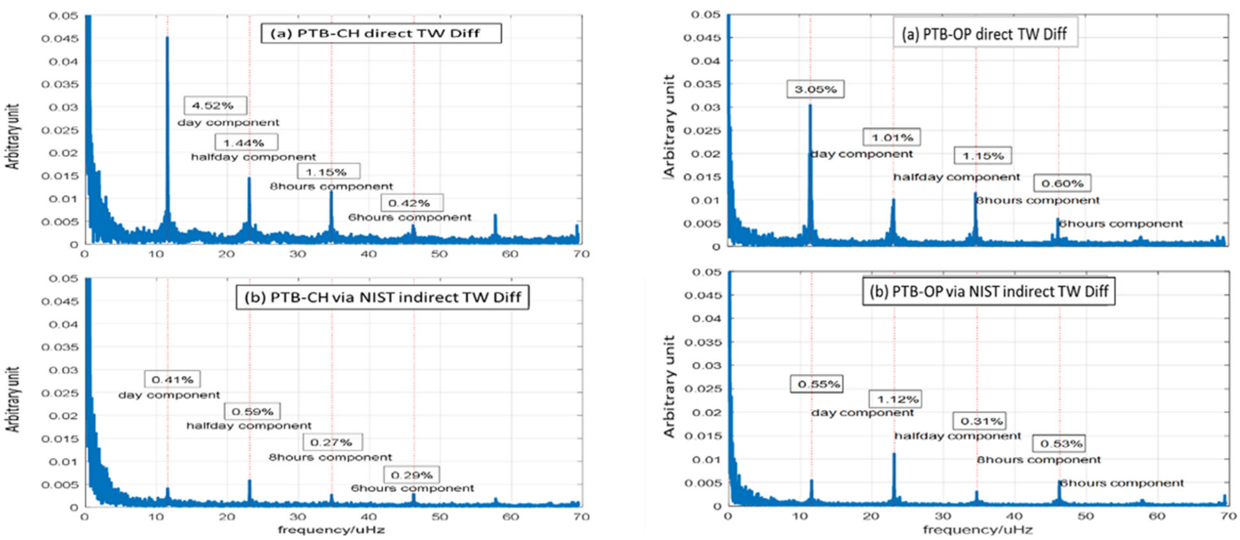

Figure 9. Spectral analysis of diurnals and other components in the Link and Links^NIST over the baselines of CH-PTB (left) and OP-PTB (right). The components of the TWSTFT differences are presented with an arbitrary unit because we are only interested in the comparison of the diurnal reduction of the indirect link relative to the direct link. The OP-PTB spectral analysis data are taken from [12].

*4.2. Indirect SATRE TWSTFT link: Link^*

4.2.1. Consistency in the calibrations of the direct and indirect links: Link versus Link^. The inner-Europe links were mostly calibrated using TWSTFT mobile stations while the transatlantic links were calibrated with the BIPM's traveling GPS calibrator and the USNO TWSTFT mobile station (for USNO-PTB baseline). We assume that the direct link, Link (Lab1 – Lab2), and the indirect link, Link^ (Lab1_Lab2^Lab3), have been both calibrated, the time transfer results of Link should agree to that of Link^. We expect the difference in the two types of links is within u_A (0.5 ns) for TWSTFT. The differences should be as small as possible. The consistency can be verified by studying the DCD(Link–Link^)

Table 4. (a) The gain factor of the diurnal reduction in the Links^NIST versus the Link. (b) The gain factor of the diurnal reduction in the Links^USNO versus the Link.

(a)

Baseline	PTB-CH	PTB-IT	PTB-OP	PTB-ROA	PTB-SP	**Mean**
Gain factor	3.3	1.6	2.3	1.8	1.7	**2.14**

(b)

Baseline	PTB-CH	PTB-IT	PTB-OP	**Mean**
Gain factor	2.7	1.3	1.8	**1.93**

Table 5. Comparing GPSPPP to the TWSTFT direct link and the indirect links via SP, NIST or USNO.

Baseline	N	σ(DCD)/ns	σ(DCD^SP)/ns	σ(DCD^NIST)/ns	σ(DCD^USNO)/ns	Gain ^SP = (3)/(4)	Gain ^NIST = (3)/(5)	Gain ^USNO = (3)/(6)
(1)	(2)	(3)	(4)	(5)	(6)	(7)	(8)	(9)
CH-PTB	335	0.61	0.74	0.23	0.24	0.77	2.7	2.5
IT-PTB	365	0.81	0.95	0.43	0.53	0.85	1.9	1.5
OP-PTB	355	0.43	0.53	0.20	0.35	0.81	2.2	1.2
ROA-PTB	335	0.83	0.82	0.41	0.39	1.01	2.0	2.1
SP-PTB	360	0.54	—	0.25	0.29	—	2.2	1.9
VSL-PTB	370	0.56	0.67	0.43	0.35	0.84	1.3	1.6
Mean						**0.85**	**2.1**	**1.8**

over the same baseline. In DCD, the clock performance would not be completely cancelled if the two measurements used in DCD are made at different time due to the measurement schedule involved. We interpolate the DCD data sets such that the Link and Link^ are aligned at the same timestamps.

Table 2 gives the statistics of DCD(Link–Link^) for six UTC baselines in Europe. The indirect links are relayed by NIST and USNO in the USA. The data used are between MJDs 57414 and 57446. *N* is the number of the data epochs used. All involved laboratories are equipped with Hydrogen Maser clocks as references for the TWSTFT ground stations (and GPS receivers) except for VSL where a Caesium clock is employed. The maximum discrepancy is 0.462 ns over the baseline of VSL–PTB, which could be at least partly attributed to the noise of the Caesium clock at VSL, but it is still below the conventional TWSTFT link measurement uncertainty $u_A = 0.5$ ns. The mean value of Link^NIST and Link^USNO is 22 and 33 ps, respectively, which are statistically consistent with zero ns. This confirms that calibrations of Link and Link^ are fully consistent no matter which of the relaying stations is used. We want to point out that the calibrations were not performed at the same time.

4.2.2. Improvements in reducing the instability and the diurnal: Link versus Link^. In this section, we quantify the improvement of indirect links with respect to direct links through different indicators: TDev, FFT, DCD using PPP/IPPP as reference and relaying by different laboratories.

4.2.2.1.Time deviation analysis. We use TDev to study the gain factors in reducing the diurnal and the instability on different averaging times.

Figure 8 is the TDev of the direct (blue) and indirect (red) link over the baseline of OP-PTB. The TDevs are obtained by using three years' continuous data between 2014 and 2016 [12]. The diurnal is greatly reduced and stability is significantly improved for averaging times up to 2 d. Longer averaging reveals the properties of the two time scales involved.

Tables 3(a) and (b) are based on the datasets of MJDs 57419–57447 for the baselines of CH-PTB and OP-PTB. Here the gain factor for each averaging time of 2, 4, 8, 16 and 32 h are given. As shown in the tables, the gain factors for the baseline of CH-PTB are correspondingly 2.9 and 2.3 for the indirect links via NIST and USNO. For the baseline of OP-PTB, the gain factors are 2.6 and 2.7 for the indirect link via NIST and USNO. On average, the gain factors are 2.8 for NIST and 2.5 for USNO, respectively.

4.2.2.2.Spectral analysis. Spectral analysis of the diurnal (day component) and other components in the direct and indirect SATRE TWSTFT links are obtained using FFT. Three years (2013–2015) of data were analysed.

Figure 9 shows examples of the results for the UTC baselines of CH-PTB and OP-PTB. The diurnal in the Link (direct links) is noticeably reduced in the Link^NIST. The other components are also reduced, except for the half-day component, which is slightly increased in the OP_PTB^NIST.

Table 4(a) gives the gains for five European indirect links via NIST. The gains are computed from $\sqrt{}$ [(day component of Link)/(day component of Link^)]. The minimum gain factor is 1.6 (IT_PTB^NIST) and the maximum is 3.3 (CH_PTB^NIST). The mean value of the gains is 2.1. The diurnals in the indirect link are indeed reduced with respect to that in the direct links. To check if the diurnal reduction is dependent on the relaying station in the USA, we additionally computed the gains of CH_PTB^USNO, IT_PTB^USNO and OP_PTB^USNO. From table 4(b), we see these Links^USNO also produce a diurnal reduction at similar levels to that of Links^NIST. The mean value of the gains is 1.9 for Links^USNO. By the FFT analysis, we achieve the same conclusion given by the TDev analysis in the last section.

4.2.2.3.Comparison to GPSPPP and the role of the relaying station in the SATRE TWSTFT Link^. Taking GPSPPP as the reference of the comparisons, table 5 lists the gain factors of the six inner-European indirect links versus the direct links for the corresponding relaying laboratories SP, NIST and USNO. The mean gain factors are 0.85, 2.1 and 1.8, respectively. Note that when a gain factor is smaller than 1, there is a loss and this is the case of the Link^SP (0.85). In fact, we tested each of the stations in the Europe-to-Europe and Europe-to-USA network as the relaying station and conclude that the diurnal in the Europe-to-Europe SATRE TWSTFT cannot be reduced by using a European relaying station. Our analysis shows the diurnals in the direct Europe-to-Europe SATRE TWSTFT links can be reduced by the indirect links using a relaying

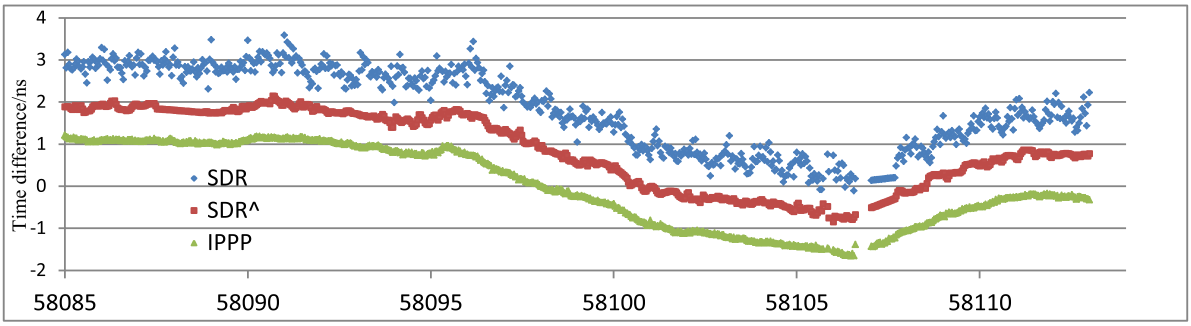

(a)

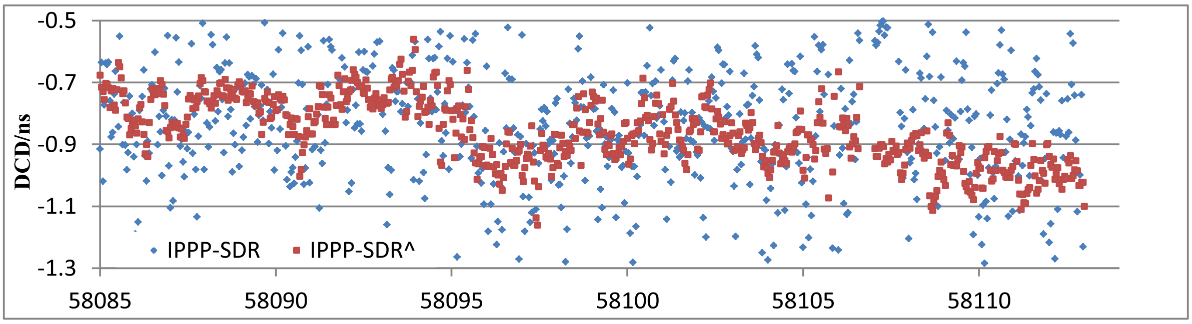

(b)

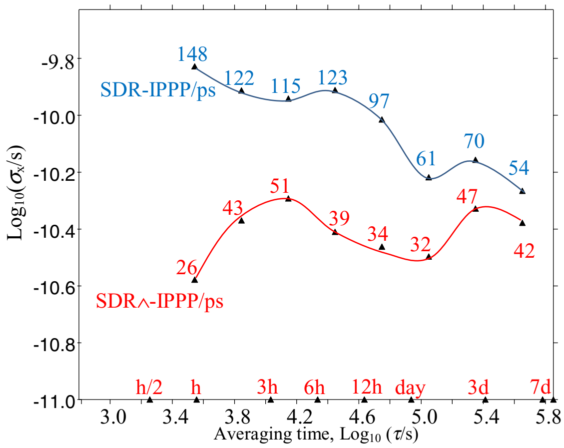

(c)

Figure 10. (a) The SDR, SDR^ and IPPP links over the baseline of OP-PTB. The results are offset for demonstration purpose. (b) The DCD(IPPP – SDR) with $\sigma = 0.221$ ns and DCD(IPPP – SDR^) with $\sigma = 0.106$ ns, corresponding to figure (a). (c) TDev of the DCD_{SDR} and $DCD^{\wedge}_{SDR}$ corresponding to figure (b). The axes of the plot are in log scales. The numbers in the plot represent σ_x values in picoseconds.

Table 6. Gain factors for the TDev of DCD_{SDR} and $DCD^{\wedge}_{SDR}$ corresponding to figure 10(c).

Averaging time (h)	DCD_{SDR} σ_x/ns	$DCD^{\wedge}_{SDR}$ σ_x/ns	Gain = (2)/(3)
(1)	(2)	(3)	(4)
1	0.148	0.026	5.7
2	0.122	0.043	2.8
4	0.115	0.051	2.3
8	0.123	0.039	3.2
16	0.097	0.034	2.9
32	0.061	0.032	1.9
64	0.070	0.047	1.5
Mean			**2.9**

Table 7. Gain factors in indirect SDR^ versus direct SDR with IPPP as reference and NIST as relaying station.

Baseline	$\sigma(DCD_{SDR})$/ns	$\sigma(DCD^{\wedge}NIST_{SDR})$/ns	Gain = (2)/(3)
(1)	(2)	(3)	(4)
OP-PTB	0.221	0.106	2.1
AOS-PTB	0.206	0.145	1.4
AOS-OP	0.346	0.136	2.6
Mean	**0.258**	**0.129**	**2.0**

station in the USA. The study in [12] strongly suggested the dominant cause of diurnals in the Europe-to-Europe SATRE TWSTFT is related to the in-band TWSTFT signal interference and properties of the receive part in the SATRE modem (see section 6 for a more detailed discussion). On the other

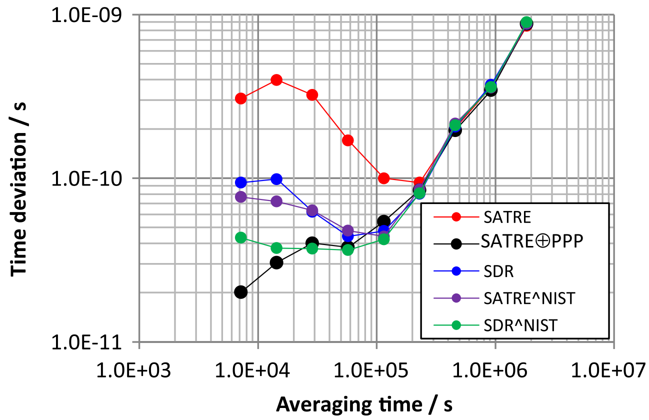

(a)

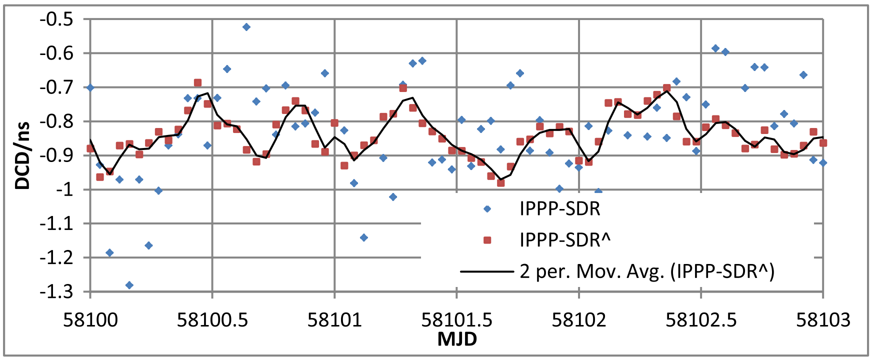

(b)

Figure 11. (a) Comparison of TDev for different TWSTFT links over the baseline of OP-PTB. (b) Enlarged three-day segment of figure 10(b), the DCD(IPPP – SDR) and DCD(IPPP – SDR^NIST) over the baseline of OP-PTB.

Table 8. Gain in TDev of the direct SDR link against the indirect link (Link^NIST) of SATRE and SDR over the baseline of OP-PTB.

Average time (h)	SATRE^ σ_x/ns	SDR σ_x/ns	SDR^ σ_x/ns	SDR versus SATRE^ gain = (3)/(2)	SDR versus SDR^ gain = (3)/(4)
(1)	(2)	(3)	(4)	(5)	(6)
2	0.077	0.094	0.043	1.2	2.2
4	0.072	0.099	0.037	1.4	2.7
8	0.064	0.063	0.037	1.0	1.7
16	0.048	0.044	0.036	0.9	1.2
32	0.044	0.048	0.042	1.1	1.1
Mean				**1.12**	**1.78**

hand, the gain factors achieved from using indirect links via the USA laboratories are all significant: 2.1 for ^NIST and 1.8 for ^USNO. In the table, DCD and DCD^Lab stand for DCD(Link – PPP) and DCD(Link^Lab – PPP).

4.3. Indirect SDR TWSTFT link: Link^$_{SDR}$

In this section, we always use NIST as the relaying station for SDR TWSTFT and IPPP as the reference for comparisons. The IPPP link has not been calibrated but it does not affect the results of our analysis because we only investigate the stability of Link^$_{SDR}$.

Given the above, we define DCD_{SDR} to be IPPP – SDR and DCD^$_{SDR}$ to be IPPP – SDR^. Data used in the analysis below were collected during MJDs 58085–58114. Figure 10(a) shows the differences computed with the SDR, SDR^ and IPPP links over the baseline of OP-PTB. The results are offset for demonstration purposes. Figure 10(b) is the DCD corresponding to the figure 10(a), the differences of SDR and SDR^ against IPPP. Obviously, in both figures, the SDR link is much noisier than that of the SDR^, with $\sigma(DCD_{SDR}) = 0.221$ ns and σ(DCD^$_{SDR}$) = 0.106 ns, with the gain factor 0.221/0.106 = 2.1. As illustrated in the figures, SDR^ approximates much better to the IPPP.

Figure 10(c) shows the TDev of the DCD_{SDR} and DCD^$_{SDR}$ depicted in figure 10(b). As seen in table 6, the mean gain factors due to the improvement from indirect link is 2.9. After more than three days of averaging, the gain vanishes gradually, nevertheless the residual diurnal is effectively removed.

We also computed DCD_{SDR} and DCD^$_{SDR}$ for the three baselines of OP-PTB, AOS-PTB and AOS-OP, where AOS-OP is not a UTC link. Table 7 gives the gain factors of

Table 9. Comparison of different methods against IPPP.

DCD	σ(DCD)/ns	Gain factor versus SATRE – IPPP	Gain factor versus SDR – IPPP
(1)	(2)	(3)	(4)
SATRE – IPPP	0.516	**1.0**	—
SDR – IPPP	0.158	3.3	**1.0**
SATRE^NIST – IPPP	0.131	3.9	1.2
SATRE ⊕ PPP – IPPP	0.075	6.9	2.1
SDR^NIST – IPPP	0.104	5.0	1.5
SDR ⊕ PPP – IPPP	0.078	6.6	2.0

SDR^ with respect to SDR, here IPPP is used as reference for DCD computations and NIST is the relaying station. There are significant gains in all the three baselines. The mean value of the standard deviation as a measure of instability for direct DCD_{SDR} is 0.258 ns and that of the indirect $DCD\hat{}_{SDR}$ is only half of it. The mean value of the gain factor is 2.0. Here again, considering IPPP is not error free, the gain factor may be larger than the values given in the table.

5. Comparison of different methods in diurnal reduction

We have discussed different methods for diurnal reduction in both SATRE and SDR links, using the redundancy in the UTC time transfer network, more specifically, the SDR TWSTFT, the combination of TWSTFT and GPSPPP (Link⊕) as well as the indirect links for the European UTC TWSTFT links (Link^).

Figure 11(a) compares the TDev of SATRE ⊕ PPP to that of SATRE, SDR direct links and their indirect links for the baseline of OP-PTB. The TDevs are computed from the SATRE, SDR and PPP data collected during MJDs 57645–57745. In the order of stability from the most stable to the least stable for averaging times up to 64 h, we have SATRE ⊕ PPP (black), SDR^ (green), SATRE^ (purple), SDR (blue) and SATRE (red). It is interesting and important to notice that the indirect link SATRE^ is more stable than the direct link SDR for averaging times less than eight hours. We think SDR and SATRE^ TWSTFT share some common mechanisms that cancel or reduce the diurnal from a common source. We will provide a more detailed discussion on the origin of diurnal in the next section. The SDR TWSTFT can be considerably improved with a factor about 2.0 by the SDR^ TWSTFT for averaging times up to 8 h in our examples. Although it contains more transfer noise than the SATRE ⊕ PPP for averaging times less than 8 h, the SDR^ TWSTFT is independent to GNSS time transfer and does not require extra equipment and measurements.

Table 8 gives the gains in TDev of the direct link, SDR, versus the indirect links, SATRE^ and SDR^, for different averaging times of 2, 4, 8, 16 and 32 h over the baseline of OP-PTB. The TDev values are those presented in figure 11(a). Columns (2), (3) and (4) are correspondingly the TDev on different averaging times for the links of SATRE^, SDR and SDR^. As given in figure 11(a), SATRE^ (2) is more stable than the SDR (3) with a gain factor of 1.1 on average. The most stable is the SDR^ with a gain of 1.8 on average against SDR.

Our goal is to reduce the diurnal in SATRE and SDR TWSTFT links. Table 9 is a summary of the gains in DCD standard deviation obtained using different methods. We computed the time transfer results over the baseline of OP-PTB with all the discussed techniques: SATRE, SATRE ⊕ PPP, SATRE^, SDR, SDR ⊕ PPP and SDR^. We then compare σ(DCD) and the gains. The data used were collected during MJDs 57935 to 57944. In the table, the column (1) is the list of DCD using IPPP as reference. Column (2) is the σ(DCD). Considering IPPP as the most precise technique in the listed methods, a smaller value of σ corresponds to a more precise link. Column (3) is the normalised gain factor with respect to the σ[DCD(SATRE – IPPP)] = 0.516 ns and (4) the normalised gain factor with respect to the σ[DCD(SDR – IPPP)] = 0.158 ns. Given these, the gain factors of using SDR, SDR^NIST and SDR ⊕ PPP methods over the use of SATRE TWSTFT are 3.3, 5.0 and 6.6, respectively. We want to point out that the SDR ⊕ PPP method may not be completely independent from IPPP. The gain factors of using SDR^NIST and SDR ⊕ PPP over the use of SDR are 1.5 and 2.0, respectively.

The SDR^NIST link is completely independent from the corresponding IPPP link. The stability of the SDR^ link is considerably better than that of both the SATRE and SDR links, and hence is the most precise TWSTFT result for the Europe-to-Europe UTC time transfer. Use of the SDR^ will improve the stability and the robustness of the UTC computation for Europe baselines. As discussed in section 4.2.2.3, the transatlantic NIST and USNO TWSTFT links are already available. We do not need extra equipment investment or make any extra measurements to improve the TWSTFT links.

Finally, we have shown that SDR links still contain residual diurnals which are still a dominant uncertainty source in SDR TWSTFT. On the other hand, the SDR^ links seem to be free from any diurnal pattern. In fact, if we take a closer look at the figure 10(b), the SDR^ result seems to contain some pattern, although not a diurnal. Figure 11(b) is an enlarged three-day segment of DCD(IPPP – SDR) and DCD(IPPP – SDR^) taken from figure 10(b). A second order polynomial smoothing window is used to fit the IPPP – SDR^ points. A more or less similar pattern, not a typical Random Walk, is still apparent and further study is needed. Such patterns have never been observed when comparing IPPP to more accurate techniques like optical fibre links or TW carrier phase [15, 16].

6. On the nature of diurnals

Diurnals in TWSTFT results have been investigated extensively in the past [5, 12, 18, 19, 23]. However, we still do not fully understand their dominant origin and only strategies to suppress the effect have been developed, so far. To conclude the comparison of different methods in diurnal reduction, we briefly review the sources which potentially lead to diurnals, summarize the observations made in this study, and outline the insights about the diurnals' dominant origin(s) in the Europe-to-Europe links.

The sources of diurnals (which are non-white instabilities) can be categorized by two groups. Many of them typically have a daily cycle and thus cause a diurnal pattern in the TWSTFT results. The first group is a change of the path delay difference (PDD) between the two signals travelling in opposite directions between the two ground stations, i.e. from the transmission (T_X) module of station 1 to the receiver (R_X) module of station 2 (through the ground station equipment, free space, and satellite) and in opposite direction from the T_X module of station 2 to the R_X module of station 1. The PDD can be changed by a couple of effects typically with a daily pattern:

(a) A geostationary satellite swings around its nominal position mostly due to the gravity of the sun and maneuvers for position keeping. This causes, in combination with the time offset at which the signals from the ground stations arrive at the satellite, a geometrical path delay difference. In addition, the satellite movement also changes the magnitude of the relativistic Sagnac effect;
(b) The changing exposure of different surface parts of the satellite to radiation from the sun during the day causes temperature changes also of the transponders and may lead to delay changes therein;
(c) Because the ionosphere is a dispersive medium, the signal delays to and from the satellite are slightly different for the up- and down-link signals as they are transmitted at different frequencies. The troposphere is also dispersive but at a much lower level at the used frequencies [26];
(d) The station environmental conditions, mainly temperature, but potentially also humidity and pressure may cause changes of the differential hardware delay between the T_X and R_X signal path inside each ground station.

The satellite daily movement data are not available to us and the nominal Sagnac effect of a baseline is included in the link calibration. Because the geostationary satellite is about 35 786 km above the earth surface, the daily change of PDD caused by (a) was estimated to be approximately 200 ps [23]. The effect of (b) will be canceled in the TWSTFT difference if the same transponder is used for both signal directions (such as the Europe-to-Europe links). However, the PDD change due to effect of (b) could be significant if the signals travel through two transponders (such as the Europe-to-USA links). At Ku-band frequency, the change of ionospheric delay has been estimated to be less than 150 ps [23] and the tropospheric delay would be even smaller [18]. Dependent on the quality of the earth station equipment, the environmental impact on the PPD could be as large as 1 to 2 ns.

The second group is the signal interferences from multiple transmitting stations in the TWSTFT network and potential multipath (or impedance mismatch) effects in the equipment. The interference and multipath effects cause, in combination with modem characteristics, hardly quantifiable shifts in the time-of-arrival measurements in the R_X module of each ground station. Especially the analog delay locked loops of the SATREs' R_X modules are affected at different level for the chip-rates of PRN codes used in TWSTFT. The conditions of such interferences are dependent on the instantaneous phase relations and amplitudes of the contributing signals and change dependent on the variations of signal delays along the complete signal path. The diurnal pattern of the TWSTFT results is thus similar to those from the rather systematic effects discussed above, and it is difficult to distinguish both.

We can summarize the following observations based on the analysis of the SDR and the indirect TWSTFT results: the use of SDR receivers reduces diurnals in the inner-continental, such as Europe-to-Europe, TWSTFT results. The improvement is significant but residual diurnals are still apparent. At the same time, the diurnals are only slightly reduced in the inter-continental, such as Europe-to-USA or transatlantic, TWSTFT results. Nevertheless, the indirect links between European stations via a relay station in the USA, e.g. the link OP-PTB via NIST, are unexpectedly completely diurnal-free. Moreover, the remaining scatter of the indirect link data is quite low: around or below 300 ps peak-to-peak over days, when it is compared with IPPP results. On the other hand, an indirect link OP-PTB via another European station, e.g. SP, does not give any improvement.

From the discussions above, we can obtain the following insights about the diurnal's dominant origin(s) for the Europe-to-Europe links: there are strong signal interferences in the direct TWSTFT links among European stations. These come from the simultaneous transmission of several signals through a single transponder, which is used in Europe-to-Europe links. The interferences cause diurnal shifts in the time-of-arrival measurements from the combination of code interferences and modem characteristics. The installed SDR receivers are much less sensitive to those effects compared with the analog R_X modules of the SATRE modems, leading to the observed reduction of diurnals. The remaining diurnals in the direct European links may be due to a residual impact of the still present signal interferences on the SDR correlation process and/or other changes of the PDDs as discussed above. Establishing an indirect link via another European station does not reduce the link instability. This means the conditions causing interference do not change if a European relay station is chosen. Moreover, the measurement noise is increased as expected by relaying the time scale comparison via a third station.

A brief analysis about why the indirect Europe-to-Europe links via a station in the USA can reduce diurnal has presented in section 4.2.2.3. The fact that using indirect links via NIST removes the diurnals means, that interferences are effectively suppressed by the transponder configuration for Europe-to-USA TWSTFT. For the transatlantic links two transponders are necessary, one for signals transmitted from Europe to the USA and one vice versa. Such transponder configurations are sometimes necessary to bridge very long baselines [20, 21]. The fact that the clearly apparent diurnals on the transatlantic links NIST-OP and NIST-PTB vanish by subtraction to get the indirect European link OP-PTB indicates a highly systematic nature of delay variations on the signal paths through the free space and the two transponders. Signal interferences as in Europe-to-Europe links thus have no significant impact. Also, the internal delays of both European stations at OP and PTB can be considered as less sensitive to environmental conditions because such delay variations would be present in all direct and also indirect link connections results. In summary, the concept of comparing indirect with direct links in the European-USA TWSTFT network offers the possibility to distinguish between different categories of diurnal causing effects. The method to compare such link combinations could be considered as a tool for further investigations of the diurnal's nature aiming at a better understanding and improvement of TWSTFT technique.

7. Conclusion

In the past 15 years, a diurnal variation is the most disturbing uncertainty source in TWSTFT. It is first found in SATRE TWSTFT and now the residual diurnal is found in SDR TWSTFT. Great efforts have been made to reduce its influence in UTC time transfer and we have shown that several methods can, to some level, mitigate this problem. Firstly, since 2010, the BIPM started to use a combination of SATRE TWSTFT and GPS carrier phase information [6] to successfully limit the diurnal impact in UTC computation; Secondly, the SDR TWSTFT [7–9] is an effective solution which allows one to reduce the diurnal in SATRE TWSTFT by a factor of 2–3 in most of the inner-continental links; Thirdly, for the European UTC TWSTFT links, the indirect TWSTFT links with a relaying station in the USA can greatly improve the stability of the corresponding direct SATRE links by a factor of two to three. The methods of combination of TWSTFT and GPSPPP techniques and the indirect TWSTFT links can also be used to improve the SDR links by a factor of 1.5 to 2.5. All these methods can readily be used in the present procedure of UTC to improve the stability of the contributing links.

The stability of TWSTFT (both SATRE and SDR) and GPSPPP combined links is similar and better than that of the direct SDR TWSTFT. It should be noted that the methods of SDR TWSTFT and the indirect TWSTFT are pure TWSTFT and are independent of GNSS-based techniques. Using GPS and TWSTFT time transfer results independently in UTC computation would result in a more stable and robust UTC time scale and it is envisioned to implement a rigorous formulation of such a redundant UTC link system in the future. In the future, with the development of new techniques such as the TW carrier phase and optical fibre links, the best use of the redundancy in UTC time transfer network will be a key element to improve the stability of UTC time transfer.

Acknowledgment

The authors appreciate the contributions of the TWSTFT colleagues, in particular Andreas Bauch and Shinn-Yan (Calvin) Lin for fruitful discussions.

Disclaimer

Commercial products are identified for the sake of technical clarity. No endorsement by the authors or their institutes are implied. We further caution the readers that none of the described equipment's apparent strengths or weaknesses may be characteristic of items currently marketed.

ORCID iDs

Victor Zhang https://orcid.org/0000-0002-8061-5157
Yi-Jiun Huang https://orcid.org/0000-0002-7027-9778
Dirk Piester https://orcid.org/0000-0003-2487-5613

References

[1] BIPM Circular T 360 2018 ftp://ftp2.bipm.org/pub/tai//Circular-T/cirthtm/cirt.360.html

[2] ITU Radio Communication Sector 2015 The operational use of two-way satellite time and frequency transfer employing PN codes Recommendation ITU-R TF.1153-4 (Geneva, Switzerland)

[3] TWSTFT Calibration Guidelines for UTC Time Links V 2016 ftp://tai.bipm.org/TFG/TWSTFT-Calibration/Guidelines

[4] Recommendation of the 2017 CCTF, On improving Two-Way Satellite Time and Frequency Transfer (TWSTFT) for UTC Generation www.bipm.org/en/committees/cc/cctf/publications-cc.html

[5] Zhang V and Parker T 2005 Sources of instabilities in two-way satellite time transfer *Proc. 2005 Joint IEEE Int. Frequency Control Symp. (IFCS) and Precise Time and Time Interval (PTTI) Meeting (Vancouver, Canada*, *29–31 August 2005)* pp 745–51

[6] Jiang Z and Petit G 2009 Combination of TWSTFT and GNSS for accurate UTC time transfer *Metrologia* **46** 305–14

[7] Huang Y-J, Fujieda M, Takiguchi H, Tseng W-H and Tsao H-W 2016 Stability improvement of an operational two-way satellite time and frequency transfer system *Metrologia* **53** 881–90

[8] Zhang V, Achkar J, Huang Y-J, Jiang Z, Lin S-Y, Parker T and Piester D 2017 A study on using SDR receivers for the europe-europe and transatlantic TWSTFT links *Proc. 2017 Precise Time and Time Interval Meeting—ION PTTI 2017 (Monterey, CA, 30 January–2 February 2017)* pp 206–18

[9] Jiang Z *et al* 2018 Use of software-defined radio receivers in two-way satellite time and frequency transfer for UTC computation *Metrologia* **55** 685–98

[10] Jiang Z 2008 Towards a TWSTFT network time transfer *Metrologia* **45** 6–11

[11] Tseng W H, Lin S Y and Feng K M 2008 Analysis of the Asia-Pacific TWSTFT network *Proc. IFCS* pp 487–92

[12] Zhang V, Parker T and Zhang S 2016 A study on reducing the diurnal in the europe-to-europe TWSTFT links *Proc. EFTF*
[13] Jiang Z, Zhang V, Parker T E, Yao J, Huang Y and Lin S 2017 Accurate TWSTFT time transfer with indirect links *Proc. PTTI*
[14] Jiang Z, Lin S Y and Tseng W H 2017 Fully and optimally use the redundancy in a TWSTFT network for accurate time transfer *Proc. EFTF (Besonçon, July 2017)*
[15] Petit G, Kanj A, Loyer S, Delporte J, Mercier F and Perosanz F 2015 1×10^{-16} frequency transfer by GPS PPP with integer ambiguity resolution *Metrologia* **52** 301–9
[16] Petit G, Leute J, Loyer S and Perosanz F 2017 Sub 10^{-16} frequency transfer with IPPP: recent results *Proc. 2017 Joint EFTF/IFCS* pp 784–7
[17] Riley W 2008 *Handbook of Frequency Stability Analysis* (*NIST Special Publication* vol 1065)
[18] Piester D, Bauch A, Fujieda M, Gotoh T, Aida M, Maeno H, Hosokawa M and Yang S H 2008 Studies on instabilities in long-baseline two-way satellite time and frequency transfer (TWSTFT) including a troposphere delay model *Proc. 39th Annual Precise Time and Time Interval (PTTI) Systems and Applications Meeting (Long Beach, CA, 27–29 November 2007)* pp 211–22
[19] Tseng W H, Lin H T, Chang P C, Lin S Y and Feng K M 2007 Analysis of delay fluctuations in two-way time transfer Earth stations *Proc. 39th Annual Precise Time and Time Interval (PTTI) Systems and Applications Meeting (Long Beach, CA, 27–29 November 2007)* pp 541–50
[20] Fujieda M *et al* 2011 Impact of the transponder configuration on the Asia-Europe TWSTFT network *Proc. 2011 Joint IEEE International Frequency Control Symposium & European Frequency and Time Forum (San Francisco, CA, 2–5 May 2011)* pp 655–60
[21] Fujieda M *et al* 2010 The Asia-Europe TWSTFT network using Intelsat-4 *Proc. Asia-Pacific Radio Science Conf. AP-RASC'10 (Toyama, Japan, 22–26 September 2010)* Paper AP 7
[22] BIPM KCDB CCTF-K001.UTC 2018 https://kcdb.bipm.org/AppendixD/default.asp
[23] Zhang V and Parker T 2013 A study of the diurnal in the transatlantic TWSTFT difference *2013 Asia-Pacific Time and Frequency (ATF) Workshop (Chinese, Taipei)* (https://tf.nist.gov/general/pdf/2696.pdf)
[24] Yao J and Levine J 2015 Toward continuous GPS carrier-phase time transfer: eliminating the time discontinuity at a GPS data anomaly *Proc. 28th ION GNSS + Meeting*
[25] Jiang Z, Matsakis D and Zhang V 2017 Long-term instability of UTC time links *Proc. of the 2017 Precise Time and Time Interval Meeting, ION PTTI (Monterey, CA, 30 January–2 February 2017)* pp 105–26
[26] Hobiger T, Piester D and Baron P 2013 A correction model of dispersive troposphere delays for the ACES microwave link *Radio Sci.* **48** 131–42